Measurement 88 (2016) 34–44

Contents lists available at ScienceDirect

Measurement

journal homepage: www.elsevier.com/locate/measurement

Blind equalization using combined skewness–kurtosis criterion for gearbox vibration enhancement

Jakub Obuchowski [a,*], Radosław Zimroz [b], Agnieszka Wyłomańska [c]

[a] KGHM CUPRUM Ltd., CBR, Sikorskiego 2-8, 53-659 Wroclaw, Poland
[b] Diagnostics and Vibro-Acoustics Science Laboratory, Na Grobli 15, 50-421 Wroclaw, Wroclaw University of Technology, Poland
[c] Faculty of Pure and Applied Mathematics, Hugo Steinhaus Center, Wroclaw University of Science and Technology, Wroclaw, Poland

ARTICLE INFO

Article history:
Received 7 November 2015
Received in revised form 9 January 2016
Accepted 15 March 2016
Available online 19 March 2016

Keywords:
Minimum entropy deconvolution
Blind equalization
Jarque–Bera statistic
Gearbox diagnostics

ABSTRACT

In this paper a method for vibration signal enhancement is presented. It incorporates an idea that the signal acquired on the machine housing is a convolution of an informative signal (cyclic pulse train) with an impulse response of the system. The impulse response corresponds to a transmission path through which the informative signal propagates. The informative signal is a signal that contains information about a local damage. The classical method that estimates the impulse response of the system is called minimum entropy deconvolution (MED) and it aims to maximize kurtosis of the deconvolved signal, i.e. kurtosis of the informative signal estimate. Recently, skewness-based deconvolution (equalization) has been proposed as an alternative method for damage detection in rotating machines. In this paper we incorporate an alternative criterion which combines advantages of both of the previously used deconvolution criteria. Kurtosis is a widely-used tool for impulsiveness detection even if they are hidden in the signal, although favouring single-spike signals is a disadvantage of kurtosis. On the other hand, skewness is more robust, since it incorporates statistical moment one order lower than kurtosis. However, signals related to local damage are not always asymmetric, thus skewness is not a suitable criterion for their extraction. Thus, it is worth to combine both kurtosis and skewness in a single deconvolution criterion. We compare properties of two previously used criteria (kurtosis and skewness) with the novel one which is based on the Jarque–Bera statistic using a simulation study. An experimental validation on a real vibration signal (two-stage gearbox from an open-pit mine) is performed as well.

1. Introduction

The origin of blind deconvolution algorithms driven by a measure of impulsivity is in 1978, when R.A. Wiggins developed the minimum entropy deconvolution (MED) for enhancement of seismic reflection data [1]. The method is based on searching for a linear time-invariant filter which maximizes kurtosis (normalized fourth-order statistic) of the filtered signal. Through the last decades MED has found widespread application in many areas, including machine diagnostics [2–9]. In [2] the Authors applied MED to detect localized faults in gears. Such application of MED is motivated by the fact that the faulty gear emits an impulsive signal which is often masked by other sources. MED makes the impulsive signal visible in the time domain. Moreover, MED has been validated as a useful method not only in detection of such signal, but also in advanced gear tooth localized faults diagnosis – it allows to differentiate between a spall and a crack [3]. In [4] the

* Corresponding author.
E-mail addresses: jobuchowski@cuprum.wroc.pl (J. Obuchowski), radoslaw.zimroz@pwr.edu.pl (R. Zimroz), agnieszka.wylomanska@pwr.edu.pl (A. Wyłomańska).

http://dx.doi.org/10.1016/j.measurement.2016.03.034
0263-2241/

Authors exploited MED in fault detection in rolling element bearings and guided the user to select optimum parameters for the MED filter.

The fundamental work of R.A. Wiggins has been generalized by several authors. Instead of the kurtosis one can apply other criteria of impulsivity. In [10] C.A. Cabrelli proposed a non-iterative algorithm for searching a linear filter that maximizes the D-norm, i.e. maximum absolute value of the filtered signal normalized by its Euclidean norm. An improvement of Carbelli's method that provides the same results and reduces computational time is presented in [11]. One can also benefit from generalization of the D-norm, i.e. higher order D-norms. This approach is described in [12] where the Authors analyze simulated seismic signals. Such norms might be useful in applications where an isolated impulse is expected as the excitation signal. Thus, effectiveness of this method in the field of rotating machinery diagnostics might be limited, because a set of impulses is expected in the case of damage – not only a single spike. Also, the original Wiggins' moment-based method has been extended. In [13], W. Gray analyzed normalized moments of orders other than the fourth, i.e. moments of k-th order, where $k > 2$. This generalization has been analyzed also in [12,14]. It is worth mentioning that one of these norms, namely skewness, demonstrate ability of indicating asymmetric signals which occur in certain types of damage in rotating machines [15]. In [16] the Authors provide generalization of the original minimum entropy deconvolution by incorporating so called "entropy function". In [17] the Authors introduce a method called "maximum correlated kurtosis deconvolution" (MCKD) which is desired to find a periodic series of impulses as the deconvolved signal. Another blind deconvolution method is presented in [18], where the authors propose a deconvolution norm beneficial in damage detection in planetary gearbox.

In this paper we provide another generalization of the Wiggins-type blind deconvolution algorithm. Since the previously investigated norms might be treated as measures of non-Gaussianity of the deconvolved signal, we present how the original algorithm presented in [1] might be generalized using a measure of non-Gaussianity, namely the Jarque–Bera (JB) statistic [19]. The use of this measure is motivated by several reasons. Firstly, the Jarque–Bera statistic has been recently successfully applied in rotating machinery diagnostics as an impulsivity measure that substituted the kurtosis (for some cases) in the spectral kurtosis approach [20,21]. The second reason is related to the fact that the Jarque–Bera statistic combines squares of both skewness and kurtosis. Thus, it might share kurtosis' ability of impulses detection in noisy background and skewness' properties, i.e. ability to track assymetry in the distribution of a signal and low propensity to indicate a single spike. We compare the proposed criterion with both classical MED (driven by kurtosis) and the blind deconvolution driven by skewness.

Three data sets are used in order to investigate the performance of blind equalizers. The first two are simulated signals that follow the linear time-invariant model with additive noise and noisy pulse train as excitation. One of these signals contains relatively low background noise. Moreover, variability of amplitudes of the informative signal impulses is relatively high. Thus, it could be a challenging signal for the classical MED. The second one is characterized by relatively high level of background noise. Thus, it might verify how each deconvolution criterion deals with informative signal barely visible in bot time and time–frequency domain. The third data set consists of an industrial vibration signal. Such signals are often difficult to process, especially when the related mechanical system is complex, operates in non-stationary conditions and the environment influences the measurements. For instance, measurements of instantaneous shaft's angular speed for engine diagnostics might be affected by the marine environment [22] or other types of interferences might occur during recording of the signal [23]. Non-stationary conditions might be a reason to introduce specific algorithms based on e.g. adaptive filters or time-varying models [24–26]. In general, processing of a vibration signal is only an example of challenges in industrial maintenance [27]. Thus, development of new, more robust tools for damage detection is a crucial problem in industrial data processing.

2. Methodology

Consider an input signal $\varepsilon, n = 1, \ldots, N$ (raw vibration signal). The classical version of the minimum entropy deconvolution is based on searching for coefficients $f_l, l = 1, \ldots, L$ of a filter which maximizes the following objective function of the filter's output y_n [1]:

$$O_4(f[l]) = \frac{\sum_{n=1}^{N} y^4[n]}{\left[\sum_{n=1}^{N} y^2[n]\right]^2}, \tag{1}$$

where $y_n = \sum_{l=1}^{L} f[l]\varepsilon[n-l]$. Optimal coefficients of the filter are calculated by solving

$$\frac{\partial(O_4(f[l]))}{\partial(f[l])} = 0. \tag{2}$$

Since $\frac{\partial y[n]}{\partial f[l]} = \varepsilon[n-l]$, Eq. (2) can be rewritten as:

$$\frac{\sum_{n=1}^{N} y^2[n]}{\sum_{n=1}^{N} y^4[n]} \sum_{n=1}^{N} y^3[n]\varepsilon[n-l] = \sum_{p=1}^{L} f[p] \sum_{n=1}^{N} \varepsilon[n-p]\varepsilon[n-l]. \tag{3}$$

Denoting the left side of Eq. (3) as b (cross correlation of the input and the output cubed) and the right side of Eq. (3) as multiplication of the vector f and the Toeplitz autocorrelation matrix A, Eq. (3) can be expressed as $b = fA$ (matrix form of Eq. (3)). This system might be solved iteratively. A clear description of the iterative procedure might be found in [1,2]. In the literature one can find many different criteria that define the moment to stop iterations. For instance, the iterative procedure might be stopped while a minimum change in objective function of the filter's output is reached [17], while correlation coefficient between outputs related to two following iterations is close enough to 1 [12] or while difference between filter coefficients related to two following iterations is

small enough [2]. In this paper we analyze behavior of several stopping criteria through a fixed number of iterations.

The combined skewness–kurtosis criterion that we analyze in this paper is based on the Jarque–Bera (JB) statistic. The JB statistic calculated for the output signal y_n, $n = 1, \ldots, N$ is defined as [19]:

$$JB(y) = \frac{N}{6}\left(S(y)^2 + \frac{(K(y)-3)^2}{4}\right), \tag{4}$$

where $S(y)$ and $K(y)$ are the skewness and kurtosis of the output, respectively. The JB statistic is sensitive to both skewness and excess kurtosis – any deviation from zero skewness and zero excess kurtosis increases the JB statistic. Such statistical properties are profitable especially when the blind equalization algorithm with JB statistic as the cost function is applied to a vibration signal which is leptokurtic, skew or both. The JB statistic is a special case of the LM (Lagrange multiplier) statistic used in the so-called "score test", known also as the Lagrange multiplier test. The score test can be used for testing a general class of distributions with given density function. Under the H_0 hypothesis, namely the vector of observations constitutes sample from some specific distribution, the LM statistic has asymptotically χ^2 distribution with r degrees of freedom (r – number of parameters of this distribution). The JB statistic is a particular case of LM statistic for Gaussian distribution. In our case the asymptotic distribution of JB defined as in Eq. (4) is χ^2 with 2 degrees of freedom (as the number of parameters in Gaussian distribution). It is worth mentioning that the test based on skewness and kurtosis is locally most powerful when the test statistic has form as in Eq. (4). For more details see [28]. The asymptotic distribution of JB statistic (defined as in Eq. (4)) is also discussed in [29].

On the basis of the JB statistic we propose the following objective function for blind equalization algorithm:

$$O_{JB}(f[l]) = \left(\frac{\frac{1}{N}\sum_{n=1}^{N} y^3[n]}{\left[\frac{1}{N}\sum_{n=1}^{N} y^2[n]\right]^{\frac{3}{2}}}\right)^2 + \frac{1}{4}\left(\frac{\frac{1}{N}\sum_{n=1}^{N} y^4[n]}{\left[\frac{1}{N}\sum_{n=1}^{N} y^2[n]\right]^2} - 3\right)^2. \tag{5}$$

Calculating f for which:

$$\frac{\partial(O_{JB}(f[l]))}{\partial(f[l])} = 0 \tag{6}$$

one can obtain filter coefficients for which the optimization criterion defined in Eq. (5) is maximized.

Thus, the analogous formula to Eq. (3) is:

$$\frac{C_1\sum_{n=1}^{N} y^2[n]\varepsilon[n-l] + C_2\sum_{n=1}^{N} y^3[n]\varepsilon[n-l]}{C_3} = \sum_{p=1}^{L} f[p]\sum_{n=1}^{N}\varepsilon[n-p]\varepsilon[n-l], \tag{7}$$

where:

$$C_1 = 3\frac{1}{N}\sum_{n=1}^{N} y^3\left(\frac{1}{N}\sum_{n=1}^{N} y^2\right)^2$$
$$C_2 = \frac{1}{N}\sum_{n=1}^{N} y^4\frac{1}{N}\sum_{n=1}^{N} y^2 - 3\left(\frac{1}{N}\sum_{n=1}^{N} y^2\right)^3 \tag{8}$$
$$C_3 = 3\left(\frac{1}{N}\sum_{n=1}^{N} y^3\right)^2\frac{1}{N}\sum_{n=1}^{N} y^2 - 3\frac{1}{N}\sum_{n=1}^{N} y^4\left(\frac{1}{N}\sum_{n=1}^{N} y^2\right)^2.$$

Similarly as in Eq. (3), the left side of Eq. (7) consists of weighted cross correlations and the right side is a multiplication of the vector f and the Toeplitz autocorrelation matrix A. The filter f has to be normalized (by its Euclidean norm) in every iteration to control energy of the filter's output, thus Eq. (7) can be simplified, i.e. dividing by C_3 is not necessary. $\frac{1}{N}\sum_{n=1}^{N} y^k$ is the k-th order moment and $\sum_{n=1}^{N} y^k[n]\varepsilon[n-l]$ is the cross correlation of the input and the output to the power k. Eq. (7) might be solved for f using the standard iterative algorithm described in [1]. As it is mentioned in [30], the recommended way of calculating cross correlations is based on the Wiener-Khinchin theorem, i.e. using the Fast Fourier Transform (FFT) and its inverse (IFFT). Benefits from using FFT and IFFT are clearly perceptible when the order of the filter is large and the input signal is long.

In order to provide comprehensive analysis, we compare the results obtained using kurtosis and JB statistic as criteria with the blind deconvolution driven by one of Gray's variability norms, that incorporates normalized third statistical moment (skewness). The objective function is defined as [13]:

$$O_3(f[l]) = \frac{\sum_{n=1}^{N} y^3[n]}{\left[\sum_{n=1}^{N} y^2[n]\right]^{\frac{3}{2}}}, \tag{9}$$

where $y_n = \sum_{l=1}^{L} f[l]\varepsilon[n-l]$. Optimal coefficients of the filter are calculated by solving

$$\frac{\partial(O_3(f[l]))}{\partial(f[l])} = 0. \tag{10}$$

Eq. (10) can be rewritten as:

$$\frac{\sum_{n=1}^{N} y^2[n]}{\sum_{n=1}^{N}|y|^3[n]}\sum_{n=1}^{N}|y|^3[n]\varepsilon[n-l] = \sum_{p=1}^{L} f[p]\sum_{n=1}^{N}\varepsilon[n-p]\varepsilon[n-l]. \tag{11}$$

The left side of Eq. (11) consists of weighted cross correlation and the right side is a multiplication of the vector f and the Toeplitz autocorrelation matrix A. The iterative algorithm mentioned earlier solves Eq. (11) for f.

3. Simulated data analysis

In this section we analyze performance of blind equalizers on simulated signals, providing a motivation to incorporate a combined skewness–kurtosis criterion.

The signals we analyze are sums of response of a linear time-invariant system to an asymmetric pulse train and an additive Gaussian noise [31]. The system is characterized by its impulse response designed in order to follow properties observed in a real vibration signal from a two-stage gearbox. The asymmetric pulse train corresponds to a signal that arises in case of local damage. Duration of both signals is 2.5 s, sampling frequency is 8192 Hz and the fault frequency is 4.1 Hz. One of the signals is characterized by high level of background noise (Fig. 1, case K1) and the other one – by relatively high variability of impulses amplitudes related to local damage (Fig. 2, case K2). The noisy pulse train represents the signal that originates in a faulty gear. The linear time-invariant system represents the transmission path between the faulty gear and the accelerometer. Since the real signal related to gear fault analyzed in Section 4 is associated with more than one resonance frequency band, the linear time-invariant system is desired to consider this feature (resonance areas at 800–1200 Hz and 2500–3000 Hz). The simulated fault signal (excitation signal) is a noisy pulse train, i.e. it is a sum of a low-amplitude zero-mean white Gaussian noise and a scaled Kronecker comb function with period $P = 1998$ samples. Such period stands for fault frequency 4.1 Hz and sampling frequency 8192 Hz. The sum of Kronecker comb and a zero-mean Gaussian noise is a both asymmetric and impulsive signal. In case presented in Fig. 1 the impulses related to fault are barely-visible.

We analyze two signals related to different properties of skewness and kurtosis as criteria for blind deconvolution. The first signal (K1) is designed in order to illustrate how beneficial it could be to incorporate kurtosis in the deconvolution criterion in case of high level of background noise. This signal reveals two resonance frequency bands, although only the second band (2500–3000 Hz) is visible due to high level of noise (Fig. 3). The second signal (K2) is designed in order to present how the kurtosis-only driven deconvolution might converge to a single impulse due to relatively high variability of excitation impulses amplitudes and low level of noise. One can notice that two resonance frequency bands are clearly seen in the time–frequency map (Fig. 4).

In order to demonstrate properties of the novel deconvolution criterion we stop the iterative procedure after 160 iterations and present results of several intermediate steps, i.e. deconvolved signals after 1, 2, 3, 4, 5, 10, 20, 30, 40, 50, 100, 160 iterations. Length of the filter is set to 300 in each case. The initial filter is set as a one-sample shifted pulse. Fig. 5 illustrates how beneficial it could be to incorporate a high-order statistic (order higher than 3) in a deconvolution criterion. Recall that the occurrence of the pulse train is somehow manifested only in one of two resonance frequency bands. In this case the skewness-based equalizer could not indicate an asymmetric excitation signal even after 50 iterations (Fig. 5b). After that it tends to a single positive spike. Outputs of two other deconvolution criteria succesfully deal with a signal with high level of background noise. Both of them indicate the pulse train starting from 10 iterations and do not converge to a single pulse even after 160 iterations (Figs. 5a and c). In Fig. 6 it is demonstrated that the deconvolution driven by kurtosis tends to indicate a single spike in the deconvolved signal, beginning from the 40th iteration (Fig. 6a). This single spike is related to the second Kronecker delta of the excitation signal. Other two criteria (Fig. 6b and c) preserve the entire pulse train, even after 160 iterations. It is worth to notice that the JB-driven deconvolution converges to the pulse train faster than the skewness-based equalizer. This proves that the JB-driven equalizer could manage to indicate the pulse train properly even when one of two other analyzed criteria fail.

4. Real data analysis

In this section we analyze data that represents vibration acceleration of a two-stage gearbox operating in an open-pit mine. The gearbox transmits power from an engine to the belt conveyor driving pulley. Scheme of the gearbox and location of the accelerometer are presented in Fig. 7. Duration of the signal and sampling frequency are 2.5 s and 8192 Hz, respectively. During the measurement, rotational speed of the gearbox was almost constant, small fluctuations from the average value are negligible. Characteristic frequencies related to the damage of the first and second shaft are 16.5 Hz and 4.1 Hz, respectively. The gearbox possesses a local damage of the second shaft.

The raw vibration signal, its spectrogram and the power spectral density estimate (periodogram) are presented in Figs. 8 and 9, respectively. The signal has been also analyzed in previous works of the Authors [20,21]. One can see that majority of the power is contained in the low frequency bands, i.e. 300–400 Hz. Such energy content is related to the normal operation of the machine. The spectrogram (Fig. 9a) presents that there are cyclic impulses and they occur in 3 main frequency bands: below 300 Hz, 800–1200 Hz and 2800–3200 Hz. Such distribution

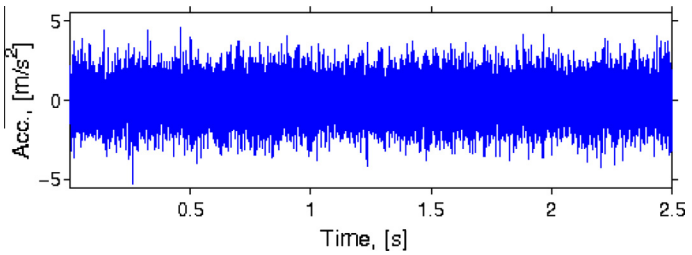

Fig. 1. Time series of simulated signal related to gear fault (case K1).

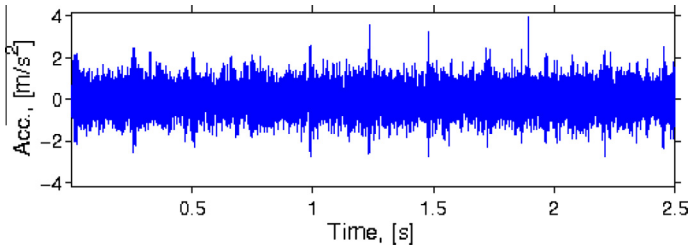

Fig. 2. Time series of simulated signal related to gear fault (case K2).

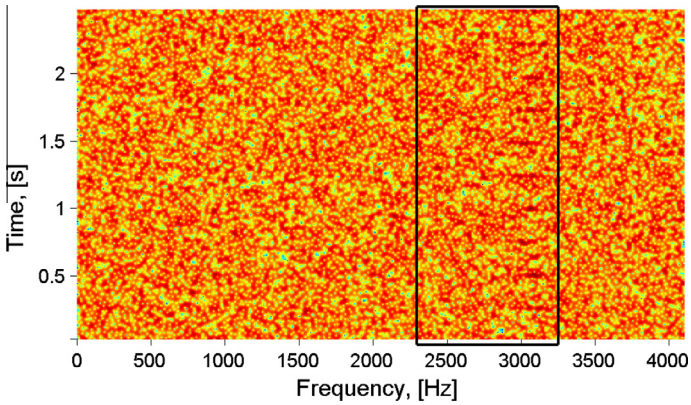

Fig. 3. Spectrogram of simulated signal related to gear fault (case K1).

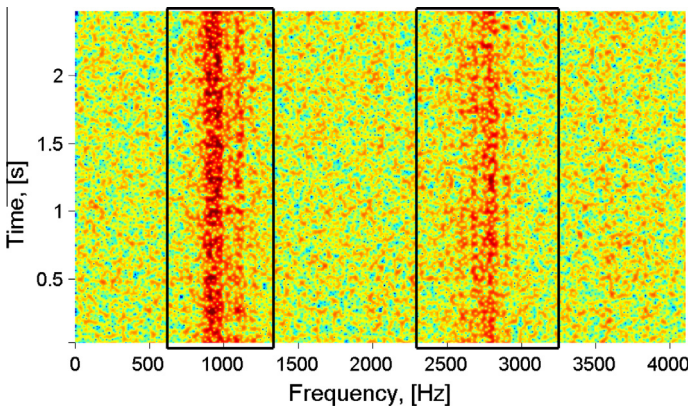

Fig. 4. Spectrogram of simulated signal related to gear fault (case K2).

of the informative frequency band might be caused by the resonance effect. While two first frequency bands contain almost every impulse that occurred during the measurement, the third one contains only a few impulses. This might be caused by random changes of the transmission path from the gear to the sensor and by small fluctuations of load. In order to make the visual analysis easier, the impulses are marked with arrows. There is also an artifact (at 0.25 s; marked with ellipses) which might affect results of methods based on quantifying impulsivity of the sub-signals from the spectrogram, i.e. the spectral kurtosis and a few of its generalizations presented in [20,21].

Fig. 10 presents values of maximized criteria as functions of the filter length and number of iterations. Note, that the log-scale is used here. Analysis of simulated signals revealed that the maximized criteria often rapidly grow through a few first iterations. Any next quick gain of a criterion value might indicate a large change of filter characteristics and thus, large change of the filtered signal. It can be noticed that in every case the maximized criterion rapidly grows through a few first iterations. One can observe that every blind equalizer fails for a certain length of the filter. Although, the JB statistic-driven equalizer reveals second rapid grow less often than MED and

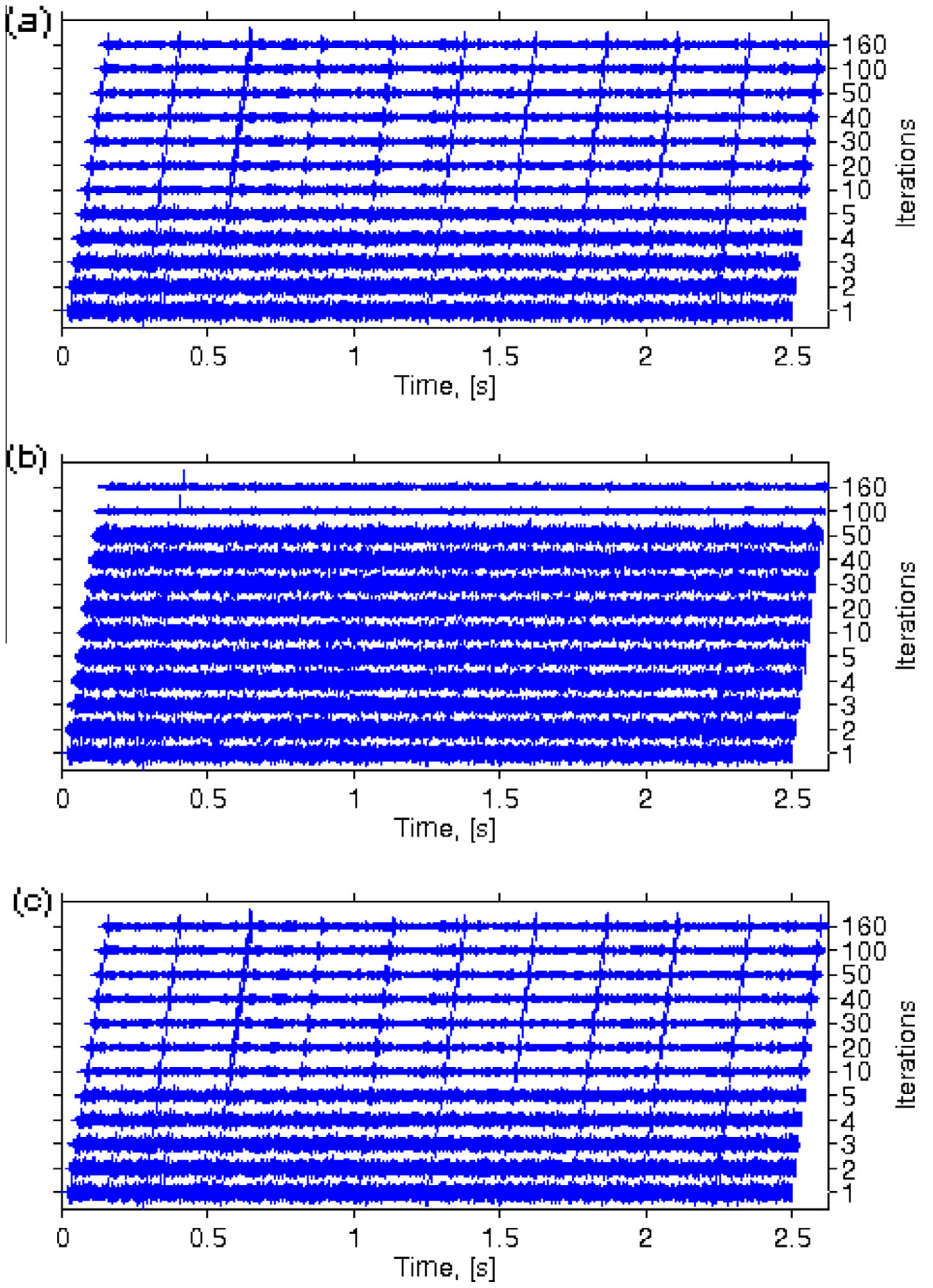

Fig. 5. Outputs of the three analyzed blind equalizers against the number of iterations. The classical MED (a), skewness-driven equalizer (b) and JB-driven equalizer (c). Case K1.

skewness-based equalizer. This indicates that the JB statistic is a better criterion for different filter lengths and it deals better with the signal contaminated with the artifact. Skewness combined with kurtosis (in JB statistic) seems to share advantages of both skewness and kurtosis.

In order to illustrate how the considered criteria perform for a given length of the filter, we analyze waterfall plots and values of maximized criteria obtained by using the filter length L equal to 80. The key results of this paper are presented in Fig. 11. The results are obtained using criteria for blind equalization described in Section 2, i.e. kurtosis (Fig. 11a), skewness (Fig. 11b) and Jarque–Bera statistic (Fig. 11c). The iterative procedure has been stopped after 200 iterations. Note that the output after first iteration is only a shifted version of the input signal, because of the initial filter f (it is a shifted pulse in time domain). It can be noticed that the outputs of blind equalization driven by kurtosis and skewness (Fig. 11a and b) converge to the artifact (at 0.25 s). Although, output of MED from 3rd to 50th is the desired pulse train related

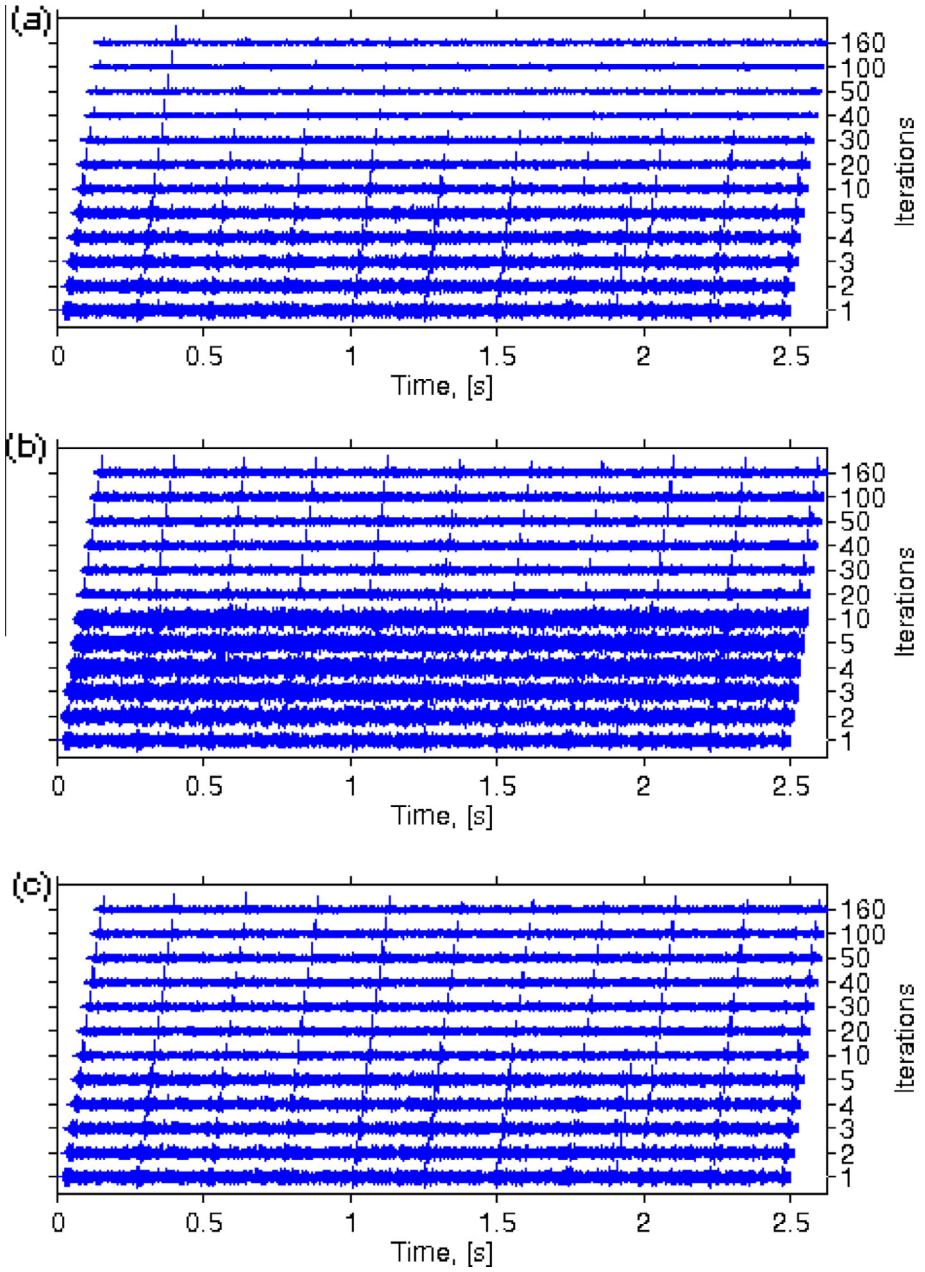

Fig. 6. Outputs of the three analyzed blind equalizers against the number of iterations. The classical MED (a), skewness-driven equalizer (b) and JB-driven equalizer (c). Case K2.

to the local damage of the gearbox. Also, a few first iterations of the algorithm based on skewness indicate the desired pulse train. Then, both of the algorithms indicate only the single pulse. In this case, the limit behavior of JB statistic-driven equalizer is significantly better, because its output converges to the pulse train – not only to the single impulse like kurtosis- or skewness-driven equalizer.

Here, we stop the algorithm after 200 iterations, in order to show how the criteria behave through certain number of iterations and to present the approximation of the limit outputs of equalizers, i.e. output signals after a large number (200) of iterations.

Fig. 12 presents that the values of the criteria might not converge monotonically or, after fast grow and temporary stabilization they might grow once again. In order to illustrate this point, we calculated values of two common criteria that define the moment to stop the iterative procedure. The first is the value of the maximized criterion (Fig. 12a, b and c) and the second is the correlation coefficient between output signals of two following iterations

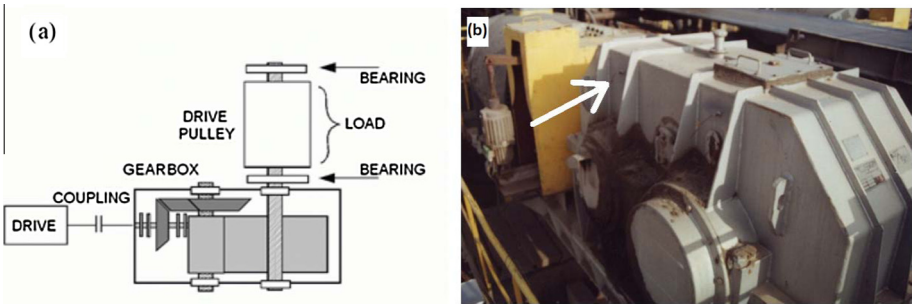

Fig. 7. Two-stage gearbox: (a) – scheme, (b) location of the accelerometer.

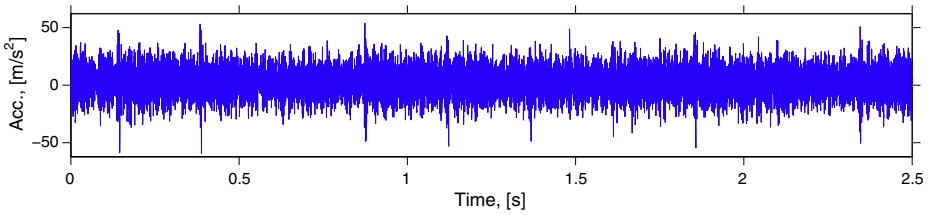

Fig. 8. Raw vibration signal from the gearbox.

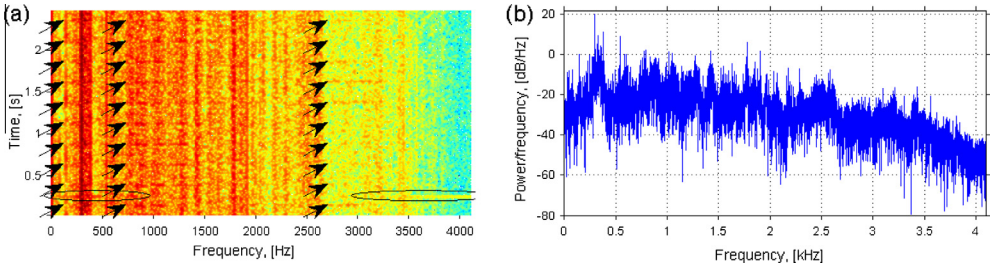

Fig. 9. Spectrogram (left panel) and periodogram (right panel) of the raw vibration signal.

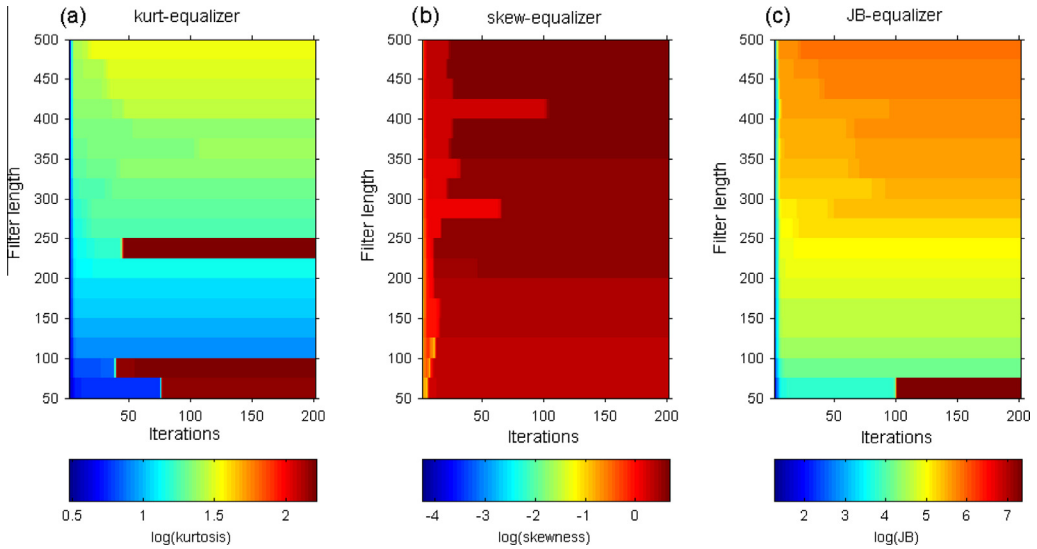

Fig. 10. Values of the criteria maximized by blind equalizers through 200 iterations versus different filter lengths (log scale): kurtosis (a), skewness (b), JB statistic (c).

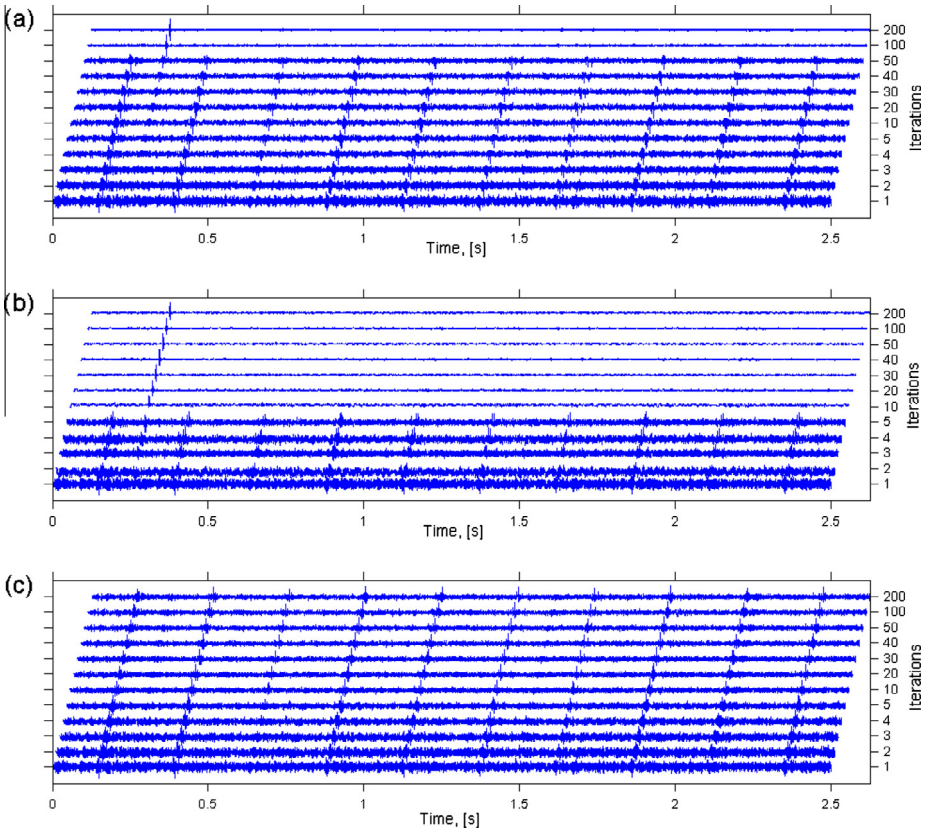

Fig. 11. Outputs of the three analyzed blind equalizers versus the number of iterations. MED (a), skewness-drive equalizer (b), JB statistic-driven equalizer (c).

(Fig. 12d). It is shown that the kurtosis of kurtosis-driven equalizer output signal grows rapidly and then it is stable from the 7th to 51th iteration. Next, it rapidly grows once again, which is related to convergence to the artifact. On one hand, increase of kurtosis through the iterations is an appropriate behavior of the iterative algorithm, since it has to find a filter that maximizes kurtosis value of the output signal. On the other hand, such indefinite maximization might be undesirable from the diagnostic point of view. The skewness-driven equalizer shares similar behavior. Skewness of the skewness-driven equalizer output grows up to the 5th iteration. This corresponds to the appropriate waterfall plot (Fig. 11b), where outputs of a few first iterations are the desired pulse train related to local damage. It cannot be said that the skewness-based filter coefficients stabilize through a certain number of iterations. Immediately after the 5th iteration, value of skewness drops till the 8th and then it rapidly gains. These inconveniences are overcame by the JB statistic-driven equalizer.

In Fig. 12c a monotonic grow and stabilization (after 10th iteration) of the maximized criterion might be observed. The stopping criterion based on the correlation coefficient indicates fast grow, drop and the next grow of correlation for skewness-based equalizer. The correlation for MED rapidly grows up to the 7th iteration, grows slowly between 8th and 51rd, then rapidly drops (local minimum at 54th iteration), grows once again and stabilizes, beginning from the 55th iteration. Behavior of JB statistic-driven equalizer is much better, i.e. it grows rapidly and stabilizes from 10th iteration. Although, a small decrease of the correlation coefficient might be observed from 3rd to 4th. Thus, this stopping criterion might provide significantly different results depending on the stopping condition. Let us denote the value of correlation coefficient at kth iteration as $C_{JB}(k)$. Firstly, while the algorithm is stopped while the C_{JB} reaches a value lower than $C_{JB}(3)$ (here, $C_{JB}(3) = 0.978$), then the output reveals barely indicated impulses (Fig. 11b). Thus, the benefit from blind equalization algorithm is minor. While a value larger than $C_{JB}(3)$ is chosen in order to stop the algorithm, then the resulting signal is the desired pulse train. On the other hand, such large threshold of the correlation coefficient would stop the skewness-based equalizer when it results in a single spike (Fig. 11b). If the iterative procedure is stopped after the first decrease of the correlation coefficient, then kurtosis- and skewness-based equalizer result in a pulse train, but then the benefit from the JB statistic-driven algorithm is minor. Thus, considering the correlation coefficient as the stopping criterion might not provide appropriate results.

Finally, we investigate the results of both equalizers after a lot (200) of iterations, what might be considered as a limit behavior. As it can be noticed in Fig. 13, the

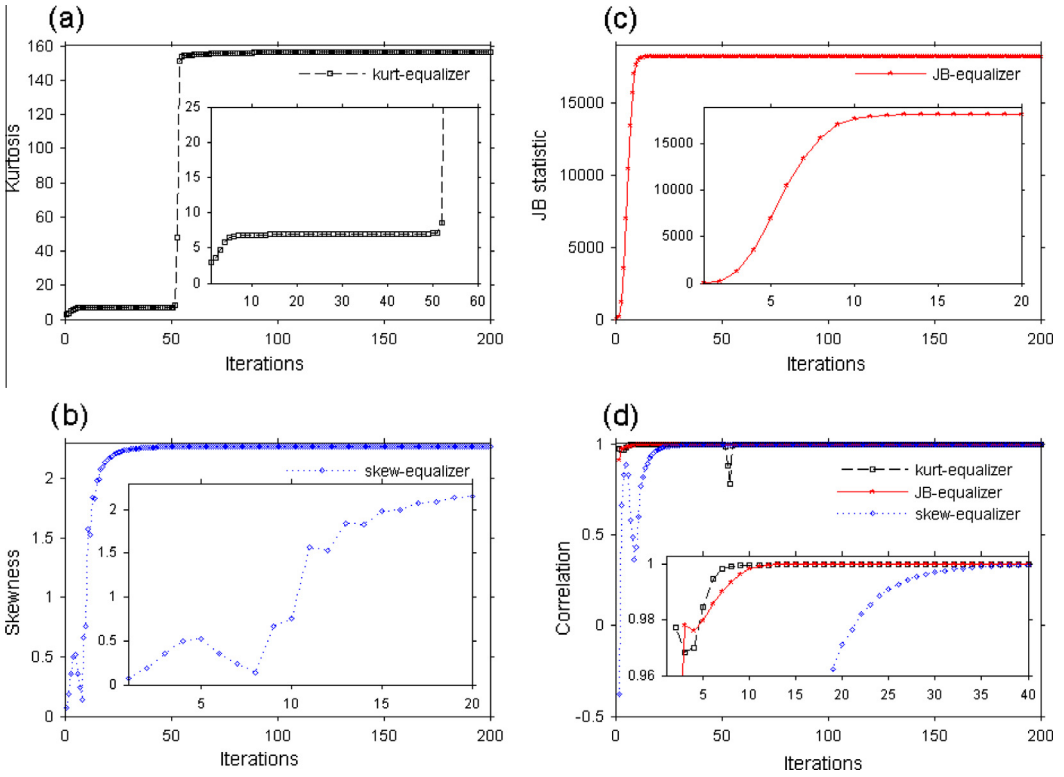

Fig. 12. Values of the criteria maximized by blind equalizers through 200 iterations (linear scale): kurtosis (a), skewness (b), JB statistic (c). Correlation coefficient between signals from two following iterations (d). Black squares (dashed line), red triangles (solid line) and blue diamonds (dotted line) are related to 3 different equalizers: MED, JB statistic-driven equalizer and skewness-driven equalizer, respectively. Analyzed signal – real data. (For interpretation of the references to colour in this figure legend, the reader is referred to the web version of this article.)

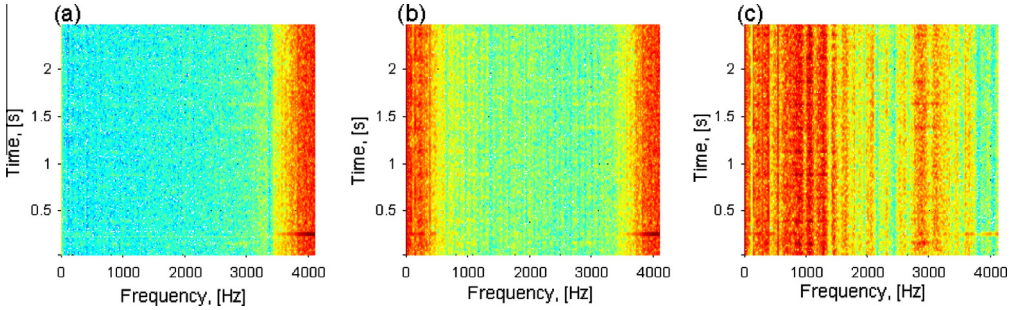

Fig. 13. Time–frequency representations (spectrograms) of signals obtained after 200 iterations of the blind equalizers based on kurtosis (a), skewness (b) and JB statistic (c).

classical MED indicates the informative frequency band located above 3700 Hz. Recall, that in this band only a single impulse appears and it is not related to condition of the machine. Likewise, the skewness-based equalizer indicate the frequency band related to the artifact. Additionally, it indicates also the lowest frequency bins (up to 500 Hz), where the artifact occurs as well. On the other hand, the JB statistic-driven equalizer indicates frequency bands related to the desired pulse train. The main energy of the resulting signal is contained between 800 and 1200 Hz. The frequency band between 2800 and 3200 Hz is also significantly indicated, but the energy is lower therein.

5. Conclusion

In this paper we presented a novel criterion for blind equalization that incorporate the Jarque–Bera statistic as the objective function. This choice is motivated by the design of this statistic, since it incorporates both kurtosis and skewness. Thus, it was expected that the JB-driven blind equalizer can indicate the appropriate excitation signal when a criterion based on a single moment (i.e. kurtosis or skewness) fails. We calculated the appropriate gradient related to the novel objective function. The new optimization criterion needs only one additional cross

correlation calculation comparing to the classical MED or other MED-type algorithms. The performance of the new criterion has been assessed using a simulation study and real data analysis. The simulation study demonstrated that equalizer based on kurtosis is beneficial in case of high level of additive noise. The skewness-driven equalizer is able to succesfully deconvolve a signal in which one impulse dominate after classical minimum entropy deconvolution. Although, each of these criteria could fail, i.e. the deconvolved signal could not be the pulse train. Kurtosis might converge to a single spike and skewness is not suitable in case of high level of noise. In order to overcome these disadvantages one can use a criterion based on both kurtosis and skewness. Simulation study revealed that the JB-driven equalizer could perform, in specific cases, at least as good as the better of these two criteria. The real data analysis provides an example when the equalizer based on the JB statistic: (a) converges faster and stabilizes for a longer time than other analyzed equalizers, (b) converges to the pulse train while others converge to the single spike and (c) reveals behavior of stopping criteria better than two other equalizers for many different filter lengths. These conclusions have been derived from analysis of both: signals obtained after a given number of iterations and values of stopping criteria through 200 iterations. Analysis of time–frequency maps after 200 iterations confirmed the preliminary observation on location of frequency bands related to both the artifact and the signal related to the gear local damage.

References

[1] R.A. Wiggins, Minimum entropy deconvolution, Geoexploration 16 (1–2) (1978) 21–35.

[2] H. Endo, R.B. Randall, Enhancement of autoregressive model based gear tooth fault detection technique by the use of minimum entropy deconvolution filter, Mech. Syst. Signal Process. 21 (2) (2007) 906–919.

[3] H. Endo, R.B. Randall, C. Gosselin, Differential diagnosis of spall vs. cracks in the gear tooth fillet region: experimental validation, Mech. Syst. Signal Process. 23 (3) (2009) 636–651.

[4] T. Barszcz, N. Sawalhi, Fault detection enhancement in rolling element bearings using the minimum entropy deconvolution, Arch. Acous. 37 (2) (2013) 131–141.

[5] N. Sawalhi, R.B. Randall, H. Endo, The enhancement of fault detection and diagnosis in rolling element bearings using minimum entropy deconvolution combined with spectral kurtosis, Mech. Syst. Signal Process. 21 (6) (2007) 2616–2633.

[6] D.-H. Kwak, D.-H. Lee, J.-H. Ahn, B.-H. Koh, Fault detection of roller-bearings using signal processing and optimization algorithms, Sensors (Switzerland) 14 (1) (2013) 283–298.

[7] R.J.G. de Oliveira, M.H. Mathias, Maximization of the signal impulsivity combining envelope technique with minimum entropy deconvolution, Appl. Mech. Mater. 392 (2013) 725–729.

[8] R. Ricci, P. Borghesani, S. Chatterton, P. Pennacchi, The combination of empirical mode decomposition and minimum entropy deconvolution for roller bearing diagnostics in non-stationary operation, in: ASME 2012 International Design Engineering Technical Conferences and Computers and Information in Engineering Conference, 24th Conference on Mechanical Vibration and Noise, Parts A and B, vol. 1, Chicago, Illinois, USA, 2012, p. 723–730.

[9] R. Jiang, J. Chen, G. Dong, T. Liu, W. Xiao, The weak fault diagnosis and condition monitoring of rolling element bearing using minimum entropy deconvolution and envelop spectrum, Proc. Inst. Mech. Eng. C J. Mech. Eng. Sci. 227 (5) (2013) 1116–1129.

[10] C.A. Cabrelli, Minimum entropy deconvolution and simplicity: a noniterative algorithm, Geophysics 50 (3) (1985) 394–413.

[11] C.-S. Wang, J. Tang, B. Zhao, Improvement on d norm deconvolution. A fast algorithm and the related procedure, Geophysics 56 (5) (1991) 675–680.

[12] M.K. Broadhead, L.A. Pflug, Performance of some sparseness criterion blind deconvolution methods in the presence of noise, J. Acoust. Soc. Am. 107 (2) (2000) 885–893.

[13] W.C. Gray, Variable norm deconvolution. PhD thesis, Stanford University, 1979.

[14] J.-Y. Lee, A.K. Nandi, Blind deconvolution of impacting signals using higher-order statistics, Mech. Syst. Signal Process. 12 (2) (1998) 357–371.

[15] A.K. Ovacikli, P. Paajarvi, J.P. LeBlanc, Skewness as an objective function for vibration analysis of rolling element bearings, in: 2013 8th International Symposium on Image and Signal Processing and Analysis (ISPA), 2013, p. 462–466.

[16] M.D. Sacchi, D.R. Velis, A.H. Cominguez, Minimum entropy deconvolution with frequency-domain constraints, Geophysics 59 (6) (1994) 938–945.

[17] G.L. McDonald, Q. Zhao, M.J. Zuo, Maximum correlated kurtosis deconvolution and application on gear tooth chip fault detection, Mech. Syst. Signal Process. 33 (2012) 237–255.

[18] B. Zhang, T. Khawaja, R. Patrick, G. Patrick, M. Orchard, A. Orchard, A novel blind deconvolution de-noising scheme in failure prognosis, Trans. Inst. Measure. Control 32 (1) (2010) 3–30.

[19] C.M. Jarque, A.K. Bera, Efficient tests for normality, homoscedasticity and serial independence of regression residuals, Econ. Lett. 6 (3) (1980) 255–259.

[20] J. Obuchowski, A. Wylomanska, R. Zimroz, Stochastic modeling of time series with application to local damage detection in rotating machinery, Key Eng. Mat. 569–570 (2013) 441–448.

[21] J. Obuchowski, A. Wylomanska, R. Zimroz, Selection of informative frequency band in local damage detection in rotating machinery, Mech. Syst. Signal Process. 48 (1–2) (2014) 138–152.

[22] M. Dereszewski, Validation of failure detection by cranckshaft angular speed analysis under sea waving conditions, Diagnostyka 15 (3) (2014) 59–63.

[23] P. Czech, G. Wojnar, R. Burdzik, L. Konieczny, J. Warczek, Application of the discrete wavelet transform and probabilistic neural networks in IC engine fault diagnostics, J. Vibroeng. 16 (4) (2014) 1619–1639.

[24] R. Makowski, R. Zimroz, A procedure for weighted summation of the derivatives of reflection coefficients in adaptive Schur filter with application to fault detection in rolling element bearings, Mech. Syst. Signal Process. 38 (1) (2013) 65–77.

[25] R.A. Makowski, R. Zimroz, Adaptive bearings vibration modelling for diagnosis, Lecture Notes in Computer Science (including subseries Lecture Notes in Artificial Intelligence and Lecture Notes in Bioinformatics), vol. 6943, LNAI, 2011, pp. 248–259.

[26] M.D. Spiridonakos, S.D. Fassois, Non-stationary random vibration modelling and analysis via functional series time-dependent ARMA (FS-TARMA) models 1 A critical survey, Mech. Syst. Signal Process. 47 (1–2) (2014) 157–224. , Mech. Syst. Signal Process. 47 (1–2) (2014) 175–224.

[27] W. Bartelmus, Object and operation supported maintenance for mining equipment, Mining Sci. 21 (2014) 7–21.

[28] C.M. Jarque, A.K. Bera, A test for normality of observations and regression residuals, Int. Stat. Rev. 55 (1987) 163–172.

[29] J. Bai, S. Ng, Tests for skewness, kurtosis, and normality for time series data, J. Business Econ. Stat. 23 (1) (2005) 49–60.

[30] M. Ooe, T.J. Ulrych, Minimum entropy deconvolution with an exponential transformation, Geophys. Prospect. 27 (2) (1979) 458–473.

[31] R.B. Randall, Vibration-based Condition Monitoring: Industrial, Aerospace and Automotive Applications, John Wiley & Sons, 2011.